The Impact of Antenna Directivity on the Small-Scale Fading in Indoor Environments

Nathan A. Goodman, *Member, IEEE*, and Kathleen L. Melde, *Senior Member, IEEE*

***Abstract*—Results obtained from using a geometrically based, single-bounce propagation model are presented to characterize small-scale fading in indoor propagation channels when directional antennas are used. The model is verified by comparing simulated results to measured results. The model is then used to obtain, via simulation, fading statistics for an indoor, line-of-sight channel. The results show that when directive antennas are used, the parameters of the Nakagami- or Rician-distributed small-scale fading vary with separation between the transmit and receive antennas. Furthermore, the strength of the variation depends on antenna directivity. Some physical mechanisms for this effect are discussed.**

***Index Terms*—Indoor propagation, , multipath fading, propagation, Rician fading models.**

I. Introduction

DIRECTIONAL antennas have the potential to significantly improve the throughput of wireless systems such as mobile *ad hoc* networks (MANET) [1], [2]. MANETs differ from traditional wireless networks that employ a centralized basestation. The mobile terminals in an *ad hoc* network function as nodes that receive and transmit data over the network. Data that is transmitted from the sender to the end user may undergo multiple hops over several nodes on the network. In [1], a medium access control (MAC) protocol that uses a separate control channel is proposed. According to this protocol, an idle node listens to the channel omnidirectionally and measures the total interference-plus-noise power. A transmitting node sends an omnidirectional request-to-send (RTS). If a receiving node wishes to accept the data packet, it switches to a directional antenna mode and responds back with a directional confirm-to-send (CTS) signal. The data is then transmitted over the network with both the transmitter and receiver using directional antenna patterns directed toward each other. When this occurs, a line-of-sight (LOS) channel with directive antennas is formed.

Generally, when no information about the directionality of the antennas is given, researchers have often assumed that the azimuthal directions of arrival of the multipath components are uniformly distributed [3], [4]. This is not the most general case, however, and a brief description of the advantages and disadvantages of different spatial propagation channel models for smart antennas is given in [2]. Several geometrically based single bounce (GBSB) models have also been developed in [5]–[8]. The GBSB models have been specifically developed for macrocell, microcell, or picocell types of environments. These models place particular assumptions on the placement of the basestation and mobile units relative to one another, but in some wireless networks, such as *ad hoc* networks, there may be no constraints on the placement of the network nodes relative to one another.

The goals of this paper are the development of a multipath fading model that accommodates directional antennas and the use of this model to quantify changes in small-scale fading as a function of antenna directivity and distance between transmitter and receiver. We present a GBSB model that has been modified in a couple of ways. First, the model allows the user to adjust the directivity of the transmit and receive antennas in order to accommodate different antennas at both ends of the channel. Second, the model also places very few constraints on the placement of the scatterers. For example, the scatterers may be located anywhere within a room rather than being confined to a geometric shape such as an ellipse or ring. The model is two-dimensional in nature in that is assumes that the multipath occurs in the same plane as the transmitter and the receiver.

After the model is verified by comparing to measured results, it is used to simulate the received signal envelope for an indoor, LOS channel. The simulated results are compared to conventional small-scale fading models that use either the Nakagami m-distribution [9] or the Rician distribution [10] for the signal envelope. The results reveal changes in small-scale fading versus transmit-receive antenna separation. These changes, which manifest themselves as changes in the parameters of the Rician and Nakagami small-scale fading distributions, are due to the varying strength of the direct signal compared to multipath components transmitted or received through antenna sidelobes. Furthermore, we find that when omnidirectional antennas are used, the small-scale fading distributions do not depend as strongly on transmit-receive antenna separation as when directional antennas are used [11], [12]. Therefore, this paper demonstrates and quantifies the relationship between small-scale fading and antenna separation as antenna directivity is increased.

The idea that small-scale fading and system performance vary with antenna directivity has been considered before. A study of path loss exponents versus antenna directivity and orientation is performed in [13]. Antenna beamwidth is considered as a factor that affects communication outage probability in [14], and [15], characterizes angle-of-arrival statistics and the Doppler spectrum for the one-ring [5], [7] model when the transmitter is directive. In [16], [17], Rician K-factors and path loss exponents were calculated from measured data. Some of the measurements

Manuscript received January 27, 2006; revised July 6, 2006.

The authors are with the Department of Electrical and Computer Engineering, University of Arizona, Tuscon, AZ 85721 USA (e-mail: melde@ece.arizona.edu).

Color versions of Figs. 1, 3, and 4 are available online at http://ieeexplore.ieee.org.

Digital Object Identifier 10.1109/TAP.2006.886530

in [16] were taken with a directional transmit antenna and some of the measurements in [17] were taken with directional antennas on transmit and receive. While there is some evidence in [17] that the Rician K-factor varies with transmit-receive separation, the analysis presented in this paper is the first to quantify the systematic relationship between antenna separation, directivity, and small-scale fading statistics.

This paper presents the results of a geometrically based single-bounce multipath model applied to small-scale fading analysis with directional antennas. The model is validated by a comparison with measured results. The model is then used to understand the effects of antenna separation on small-scale fading. This work evaluates how the separation between transmit and receive antennas affects the coefficients used in the Nakagami and Rician distributions. While other distribution functions were considered, these two distributions are well known and widely used for modeling the signal envelope in LOS channels. The Rician distribution accounts for a dominant LOS signal component, but assumes the multipath components to be approximately equal in amplitude and uniformly distributed in phase. The Nakagami distribution allows for random amplitudes and phases in the multipath components. Both distributions can be related to other probability density functions (pdfs) with the choice of appropriate parameters. They also are in forms that can be conveniently used in networking and communications simulations.

Section II summarizes the Nakagami and Rician small-scale fading distributions. Section III discusses the experimental set-up and measurement accuracy. Section IV presents the observed results from a measurement campaign of indoor channels using directional antennas. The propagation model is presented in Section V. Section VI discusses the simulation results, and Section VII presents our conclusions.

II. Small-Scale Fading Distribution Functions

Two well-known distribution functions used to characterize the received signal envelope in the presence of small-scale fading are the Rician and Nakagami distribution functions. Measured or simulated intensity results of a scattering environment can be used to determine the coefficients used in these functions. The Rician pdf is given by [10]

$$p_{rician}(r) = \frac{r}{\sigma^2} \cdot \exp\left(-\frac{r^2+\nu^2}{2\cdot\sigma^2}\right) \cdot I_0\left(\frac{r\nu}{\sigma^2}\right) \quad r \geq 0 \quad (1)$$

where r is the signal envelope, σ^2 is the variance of the signal, ν is the amplitude of the direct-path component, and $I_0(.)$ is the modified Bessel function. The coefficient $K = \nu^2/2\cdot\sigma^2$ is referred to as the Rician K-factor. Since the amplitude of the direct signal path usually cannot be measured, the value of K is usually empirically chosen. When $K = 0$, a Rayleigh distribution is obtained.

The Nakagami pdf is given by [9]

$$p_{Nakagami}(r) = \frac{2}{\Gamma(m)} \cdot \left(\frac{m}{\mu}\right)^m \cdot r^{2m-1} \cdot \exp\left(-\frac{m\cdot r^2}{\mu}\right) \quad \mathrm{r} \geq 0 \text{ and } \mathrm{m} \geq 0.5 \quad (2)$$

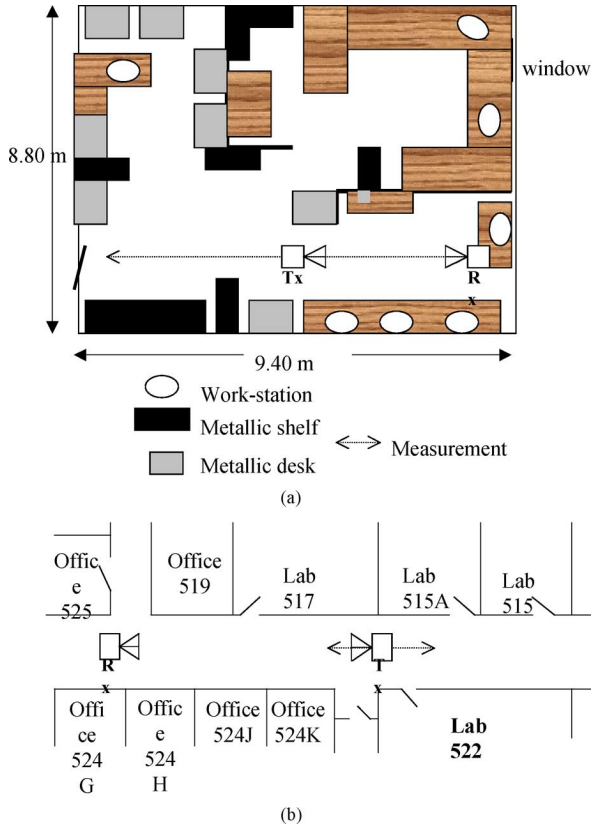

Fig. 1. Measurement site configurations (a) laboratory and (b) corridor.

where $\Gamma(.)$ is the Gamma function, μ is the average power of the received signal and m is a unitless quantity that is the inverse of the normalized variance of $r^{2\cdot}$. The parameters μ and m are given by

$$\mu = \mathrm{E}\left[r^2\right] \quad \text{and} \quad m = \frac{\mathrm{E}\left[r^2\right]}{\mathrm{var}\left[r^2\right]} \quad (3)$$

where $\mathrm{E}[.]$ represents statistical expectation. When $m = 1$, a Rayleigh distribution is obtained. Large Rician K-factors and m-factors signify strong direct-path or LOS components.

III. Experimental Set-Up

Measurements were made by recording the magnitude of the transmission parameter, S_{12}, with an HP8510C automatic network analyzer. Several diverse measurement scenarios were considered as the measurements were made in several different locations. Measurements were repeated in each case.

The measurements were made in three different locations; the laboratory of the ECE building at the University of Arizona marked with the number *522* in Fig. 1(a); the hallway corridor shown in Fig. 1(b); and a student office area comprising of cubicles with five foot high modular partitions. Fig. 1(a) shows the general layout of the laboratory that houses workstations, metallic desks, some wooden bookcases, and a small work area that is separated with partitions. The corridor is composed of laboratories on each side of a long hallway. The external walls

are concrete and the internal walls are plaster. The floor is covered with tile. In the corridor, decorative metallic strips are suspended 50 cm from the ceiling. In both the laboratory and student office setting, the ceiling is 2.7 m high and is composed of foam tiles and fluorescent lighting. In this work, it is assumed that there is only a small amount of signal penetration through the walls and the doors since the signal levels would be too small to be detected.

Detailed reports on the entire measurement campaign can be found in [11], [12]. Two different cases were measured. The first case is the short-distance line-of-sight (LOS) case that yields a strong direct signal between the transmitter and the receiver. These measurements were taken in the 522 laboratory and in the student office area. The transmit-receive separation was varied from 1.0 to 6.5 m. The short-distance LOS measurement path in the laboratory is denoted by the path labeled (1) in Fig. 1(a). The second case is a long-distance LOS case where there is a weak direct signal between the transmitter and receiver. These measurements were made in the hallway corridor and in the student office area. In both settings for the long-distance LOS scenario there is an 8.0 to 13.5 m separation between the transmit and receive antennas. In every case the antennas were aligned to achieve maximum transmission and were located one meter above the floor.

The measurements were made with an HP8510C automatic network analyzer. The receiver was placed in a fixed location and the transmitter was placed on a plastic cart. A low loss cable and power amplifiers were used to link the receive antenna to the analyzer. The amplifiers were set in order to compensate for cable loss and to ensure sufficient field strength for accurate measurements on the network analyzer. Measurements were made at 5 and 30 GHz. The 5 GHz measurements were taken with 12.6 samples per wavelength and the 30 GHz measurements were taken with 6.3 samples per wavelength.

The measurements were made using the dual exponentially tapered slot antenna (DETSA) for both transmit and receive. The DETSA was chosen since it is relatively easy to fabricate at 5 and 30 GHz, and it utilizes a simple microstrip to slotline transition and microstrip feed. The 30 GHz DETSA is a scaled version of the 5 GHz DETSA, so that the results with identical antennas could be compared. The DETSA was derived from the Vivaldi antenna, yet differs from the Vivaldi in that the outer edge of the DETSA is tapered [18]. This allows the feeds of adjacent DETSA antennas to be isolated from one another in the case of arrays or diversity antennas. The DETSA patterns are more directional than a dipole or planar inverted F antenna (PIFA). The half-power beam width in the E-plane and H-planes are 32° and 52°, respectively. The antennas were configured horizontally with the E-plane parallel with the floor.

Multiple measurements (at least three) of each different scenario were performed in order to have an adequate sampling, as there may be slight variations in measurement alignment and multipath in each case. The repeated measurements for each case and setting were intentionally done on different days and at different times of the day. No special attention was paid to "engineer" the environment to be precisely the same when different measurements were taken, although no large pieces of furniture were moved. During a measurement sweep, people did not walk around the environment. Items on the desks and workspaces may have been shifted between the measurement sweeps.

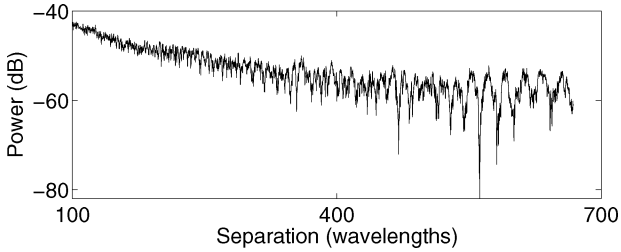

Fig. 2. Measured 30-GHz LOS signal in the laboratory setting.

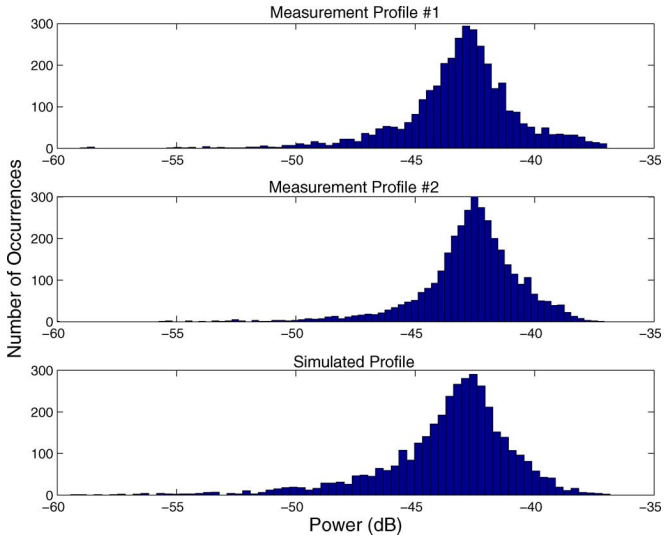

Fig. 3. Comparison of measured and simulated received-power histograms.

Fig. 2 shows one of the measured power profiles at 30 GHz made in the computer laboratory setting, and Fig. 3 shows histograms of received power for the same scenario after the path loss is removed. The top two histograms in Fig. 3 are for measured data taken over the same receiver path in the laboratory setting at two different times. The bottom histogram is for simulated data, which will be discussed further in Section V. The histograms in this form do not necessarily indicate Rician- or Nakagami-distributed fading because many of the measurements are correlated and because the LOS strength is not constant over the receive path. Full assessment of the small-scale fading pdf requires many measurements taken at different locations (with the same transmit-receiver separation) in the same environment. The repeatability of the measured results, however, does indicate that measurement accuracy was easily sufficient for the purposes of evaluating first-order small-scale fading statistics. Similar repeatability was obtained for the other measurement cases as well.

IV. Observations From Measurement Campaign

Measured results show that transmitter-receiver separation has an impact on the parameters used in the Rician and Nakagami distributions. Fig. 2 shows one of the measured signals at 30 GHz made in a computer laboratory setting when the separation between the transmit and receive antennas varied from 1 to 6.5 m. This corresponds to an antenna separation varying

from 100 to 650 wavelengths. Fig. 2 shows that when the separation between the transmit and receive antennas becomes sufficiently large, there is an apparent repetitive interference pattern. This pattern clearly shows instances of both constructive and destructive interference, thus creating large fades. The interference pattern becomes more pronounced when the transmit-receive separation becomes very large. The interference pattern is characteristic of a pattern generated from two dominant sources that are separated from one another in angle but both pointing in the direction of the receiver.

The measurement campaign described above indicated ways in which directive antennas fundamentally alter the characteristics of indoor propagation channels. Our hypothesis is that when directive antennas are used and when the transmit-receive antenna separation is small, most of the received multipath components depart and arrive through the sidelobes of the transmitting and receiving antennas. Therefore, the magnitudes of the multipath components are quite small relative to the LOS component. As the separation between the transmit and receive antennas increases, some multipath components will be received through the mainbeam or through the strongest sidelobes nearest the mainbeam of the antennas. When the transmit and receive antenna separation is large, a significant number of multipath components are received through the mainbeam of the receive antenna. When this occurs, the LOS signal is no longer dominant compared to the multipath components.

The measured results indicate that the K and m factors strongly depend on the separation between transmit and receive antennas when directional antennas are used. These results also show that the dependence of the K and m factors will decrease when less directive transmit and receive antennas are used. Unfortunately, full exploration of this relationship through a measurement campaign would require measurement of hundreds of independent LOS profiles. Therefore, the next section discusses a numerical model that was developed to further investigate the dependence of small-scale fading on antenna directivity and separation.

V. Geometrically-Based Small-Scale Fading Model

In order to fully characterize indoor wireless channels by measurement, an extensive measurement campaign is required to collect enough independent data to develop an accurate statistical representation. This, in turn, requires measurements to be taken at many different locations within the same general type of propagation environment. The resulting models are site-specific. In recent years, ray-tracing techniques have been used. These methods use a variety of reflection, diffraction, and scattering propagation models, as well as site-specific information to deterministically compute the propagation channel. These models are computationally intensive and become increasingly difficult at higher frequencies.

In order to further study the effects of antenna separation and directivity on indoor propagation models, a geometrically based single-bounce channel model was developed. This model differs from similar models presented in [2] in several ways. The models presented here apply to the more general scenario of *ad hoc* networks since no specific requirement is placed on the locations of the scatterers relative to either a basestation or mobile nodes. The model presented here includes antenna directivity as a parameter and randomly locates scatterers rather than placing them on a regular structure such as an ellipse.

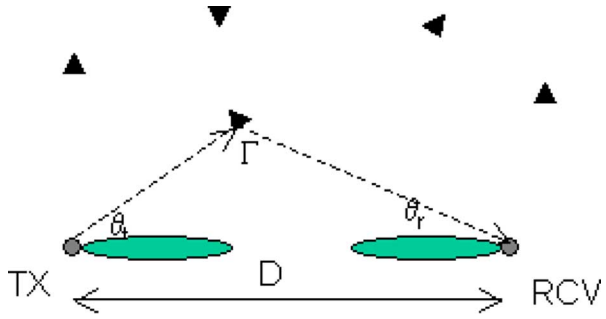

Fig. 4. Geometrically-based single-bounce channel model.

Fig. 4 shows a diagram of the model that was used. This model involves randomly placing N scatterers according to a uniform density function (the scatterers were prevented from existing along a narrow path between transmitter and receiver in order to model an unobstructed LOS). The randomly located scatterers represent arbitrary configurations of desks, bookcases, and other objects typically found in an indoor environment. Each scatterer was also given a random scatterer reflectivity (Γ) according to a Rayleigh distribution in amplitude and a uniform distribution in phase. This model is used to simulate the received signal envelope. The form of the single-bounce model used in this work is

$$s = g_t(\theta_{tLOS})\frac{e^{-jkR_{LOS}}}{R_{LOS}}g_r(\theta_{rLOS}) + \sum_{n=1}^{N} g_t(\theta_{tn})\frac{e^{-jkR_{tn}}}{R_{tn}}\Gamma_n\frac{e^{-jkR_{rn}}}{R_{rn}}g_r(\theta_{rn}) \quad (4)$$

where N is the number of scatterers, θ_{tn} is the angle of departure between the transmitter and the n^{th} scatterer, θ_{tLOS} is the angle of departure between the transmitter and receiver, θ_{rn} is the angle of arrival between the receiver and the n^{th} scatterer, θ_{rLOS} is the angle of arrival between the transmitter and receiver, $g_t(\theta_{tn})$ is the far-field pattern of the transmit antenna in the direction of the n^{th} scatterer, R_{tn} is the distance between the transmit antenna and the n^{th} scatterer, Γ_n is the reflectivity of the n^{th} scatterer, $g_r(\theta_{rn})$ is the far-field pattern of the receive antenna in the direction of the n^{th} scatterer, R_{rn} is the distance between the n^{th} scatterer and the receive antenna, and R_{LOS} is the transmitter-receiver separation. The expression given in (4) is similar to modeling radar propagation and assumes that the antennas are polarization matched. For our simulations, N was set to 100.

In order to verify the model, the simulation of a physical scenario was compared to one of the LOS measurement collections described in Section III. The measurements contained a periodic interference pattern similar to the pattern in Fig. 2. After evaluating the interference pattern and the laboratory layout, it was determined that the interference was probably due to a dominant multipath component reflecting off a metallic desk. This

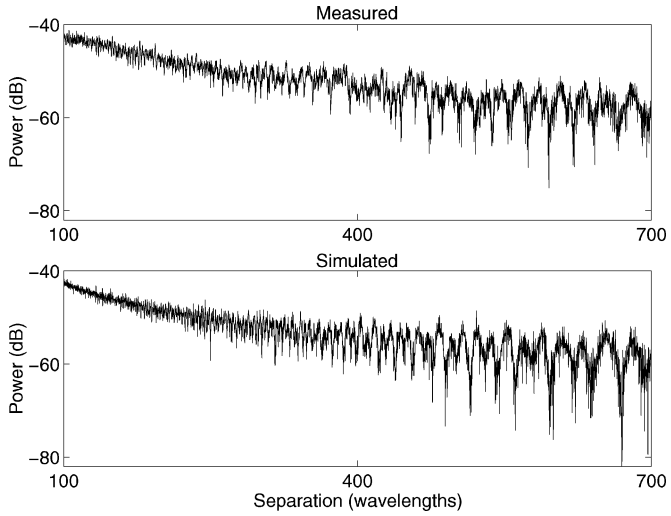

Fig. 5. Comparison of measured and simulated power profiles.

constraint was enforced in the simulation, which resulted in received signal components due to the (unobstructed) direct path, the dominant multipath component, and many other randomly located scatterers. The additional scatterers were randomly located within the room according to a uniform density with the exception of a 1-m, unobstructed swath along the system's LOS.

Fig. 5 compares measured and simulated signal power as a function of the separation between transmit and receive antennas. The two power profiles have the same relative level and similar pattern characteristics. Both power profiles fluctuate very little when the antennas are close due to a dominant LOS component. When the antennas become separated, however, the dominant multipath component propagates through the major sidelobes and eventually the antenna mainlobes, giving rise to the periodic interference pattern. A histogram of the simulated received power after removing the effects of path loss is shown in the bottom plot of Fig. 3 where it can also be seen that the histogram agrees very well with those obtained through the measurement campaign. Only two components of the propagation environment (the direct path and the dominant multipath) were deterministically modeled in this example. Yet despite the simple nature of this simulation compared to ray-tracing approaches, the comparisons between the two power profiles are excellent.

VI. Results

In this section, simulations using the model in (4) were used to evaluate properties of small-scale fading in indoor, LOS environments similar to what might be found in academic or office buildings. Isolated rooms were considered since at 30 GHz the signal does not efficiently propagate through walls or other barriers. Monte Carlo simulations were performed in an environment based on a configuration similar to the one in Fig. 4. Scatterers were randomly distributed within an 8.8 by 9.4-m room except for a 1-m swath along the LOS path. This last constraint was applied to enforce an unobstructed LOS requirement. The scattering coefficients for the scatterers were randomly generated according to a Rayleigh distribution in amplitude and a uniform distribution in phase.

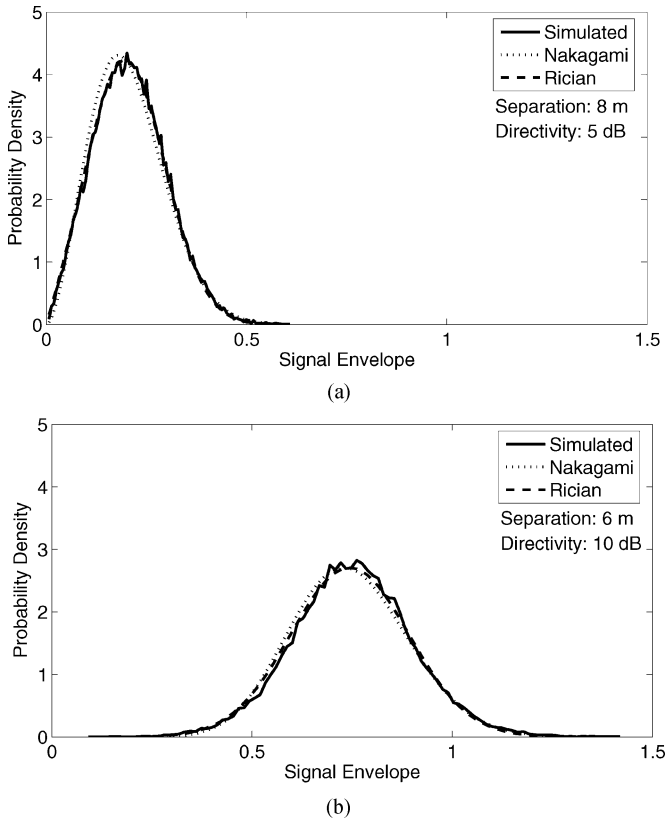

Fig. 6. Comparison of simulated and theoretical pdfs for two different LOS scenarios.

We generated fading statistics for the received signal envelope at transmitter-receiver separations ranging from 2 to 8 m. At each antenna separation, 30,000 trials were performed. For each trial, we generated new scatterer locations and reflection coefficients, and the outcome of each trial was the received power level resulting from the coherent combination of the LOS and all multipath components. By generating new scatterer locations for each trial, we were able to generate 30,000 statistically independent signal envelopes designed to represent the endless number of configurations that could be observed for the same type of propagation environment (in this case, an indoor academic laboratory and study area). After the trials were performed, a numerical pdf was generated from the results and compared to the Nakagami and Rician distributions. The parameters of the distributions were varied to find the best fit as measured by the relative entropy between the two pdfs [19]. The process is then repeated for varying separation and antenna directivity.

Antenna directivity was controlled by raising the azimuthal power pattern to a power and then normalizing the results to have constant effective isotropic radiated power. Let the pattern of the DETSA antenna be denoted as $P(\theta)$. Then the various directive antenna patterns were obtained by

$$G(\theta) = AP^x(\theta) \tag{5}$$

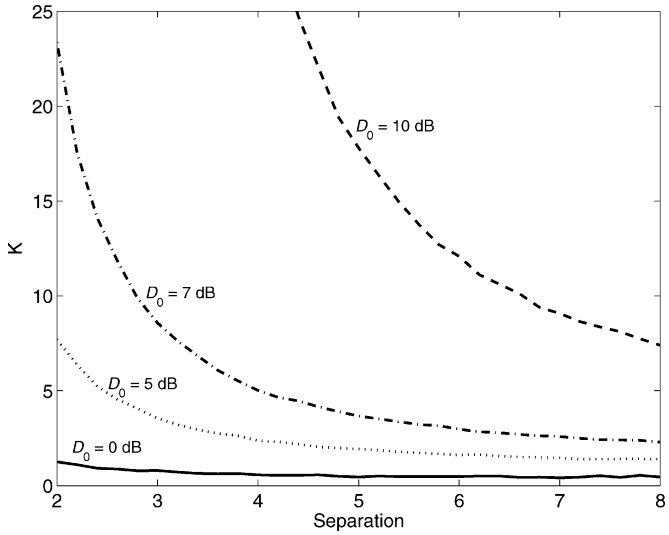

Fig. 7. Rician K-factor as a function of antenna separation for different antenna directivities.

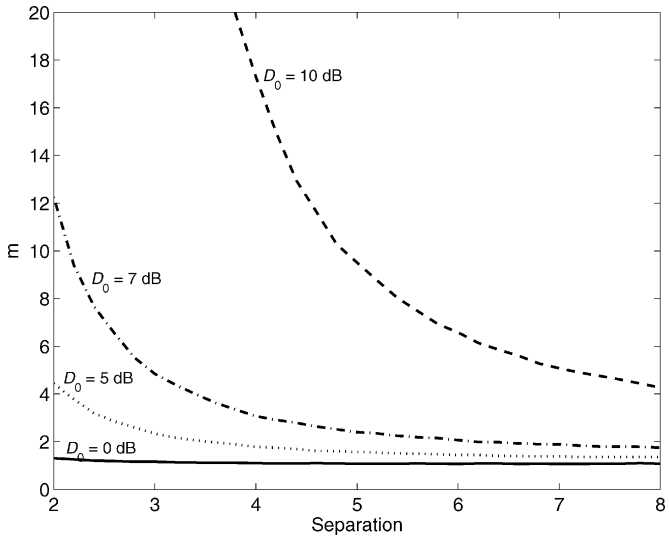

Fig. 8. Nakagami m-factor as a function of antenna separation for different antenna directivities.

where $x \geq 0$ controls directivity by modifying the shape of the DETSA pattern and the constant A normalizes the total radiated power. When $x = 0$, the pattern is omnidirectional.

Fig. 6 shows two examples of the pdf fit for two different transmit-receive separations and antenna directivities. In Fig. 6(a), the separation is 8 m and the antenna directivity for both antennas is 5 dB. In Fig. 6(b), the separation is 6 m and the directivity is 10 dB. Since the antennas in Fig. 6(b) are closer and more directive, the LOS component is stronger compared to multipath than in Fig. 6(a). In Fig. 6(a), the distribution looks similar to a Rayleigh distribution, which is used for non-LOS environments.

Figs. 7 and 8 clearly show how the Rician K-factor and Nakagami m-factor vary as a function of antenna separation. For small separation, only the LOS component propagates through the antenna mainlobes; hence, the LOS component is very dominant, which results in large K (Fig. 7) and m (Fig. 8) values. For large separation, it is possible for a signal to depart from the transmitting mainlobe, to reflect off a scatterer, and to arrive through the receiving mainlobe. Therefore, many multipath components compete with the LOS component, the LOS component is less dominant, and small K and m values are observed. Furthermore, Figs. 7 and 8 demonstrate that as antenna directivity increases, the strength of the relationship between antenna separation and K or m increases. For omnidirectional antennas ($D_0 = 0$ dB in Figs. 7 and 8), K and m vary little with separation. This is because no propagation path is preferred by the transmitting and receiving paths. For highly directive antennas, however, K and m start small at 8-m separation but rapidly increase as separation is decreased.

VII. Conclusion

This paper discusses a geometrically-based single-bounce simulation model that was used to compare how the values of K in a Rician distribution, and the values of m for a Nakagami distribution are affected by antenna directivity for small scale fading of indoor wireless channels. The Nakagami and Rician distributions both work well for indoor wireless channels with directive antennas because both distributions have factors that can be varied with antenna directivity. The simulation results have been compared with measured results. The simulation results show that the K and m-factors vary exponentially with distance for LOS channel with directive elements. These results can be used to properly design and configure LOS wireless links through proper choice of antenna directivity and separation.

References

[1] A. Arora and M. Krunz, "Power-controlled medium access for ad hoc networks with directional antennas," *Ad Hoc Networks J.*, to be published.

[2] J. Liberti and T. S. Rappaport, *Smart Antennas for Wireless Communications: IS-95 and Third Generatuion CDMA Applications*. Englewood Cliffs, NJ: Prentice-Hall, 1999.

[3] M. J. Gans, "A power spectral theory of propagation in the mobile radio environment," *IEEE Trans. Vehic. Tech.*, vol. VT-21, pp. 27–38, Feb. 1972.

[4] J. D. Parsons, *The Mobile Radio Propagation Channel*. New York: Wiley, 1992.

[5] W. C. Jakes, *Microwave Mobile Communications*. New York: IEEE Press, 1994, IEEE Press Classic Reissue.

[6] R. B. Ertel and J. H. Reed, "Angle and time of arrival statistics for circular and elliptical scattering models," *IEEE J. Select. Areas Commun.*, vol. 17, no. 11, pp. 1829–1840, Nov. 1999.

[7] R. B. Ertel, P. Cardieri, K. W. Sowerby, T. S. Rappaport, and J. H. Reed, "Overview of spatial channel models for antenna array communication systems," *IEEE Personal Commun.*, vol. 5, no. 1, pp. 10–22, Feb. 1998.

[8] R. Janaswamay, *Radiowave Propagation and Smart Antennas for Wireless Communications*. Norwell, MA: Kluwer Academic, 2001.

[9] M. Nakagami, "The m-distribution – A general formula of intensity distribution of rapid fading," in *Statistical Wave Methods in Radio Wave Propagation*, W. C. Hoffman, Ed. New York: Pergamon Press, 1960, pp. 3–35.

[10] T. S. Rappaport, *Wireless Communications Principles and Practices*. Englewood Cliffs, NJ: Prentice-Hall, 1996.

[11] D. Beauvarlet and K. L. Virga, "Measured characteristics of 30 GHz indoor propagation channels with low-profile directional antennas," *IEEE Antennas Wireless Propag. Lett.*, vol. 1, pp. 87–90, 2002.

[12] K. L. Virga, C. Hammond, D. Beauvarlet, and W. E. Ryan, "Indoor propagation measurements using low profile and directional dual exponentially tapered slot antennas," in *Proc. IEEE 5th Int. Symp. Wireless Personal Multimedia Communications*, Oct. 2002, pp. 193–197.

[13] A. H. Wong, M. J. Neve, and K. W. Sowerby, "Performance analysis for indoor wireless systems employing directional antennas," *Proc. Inst. Elect. Eng. Commun.*, vol. 152, no. 6, pp. 890–896, Dec. 2005.
[14] P. C. Yeh, W. E. Stark, and S. A. Zummo, "Outage probability of wireless networks with directional antennas," in *Proc. IEEE Military Commun. Conf.*, Monterey, CA, 2004, vol. 1, pp. 333–338.
[15] P. Petrus, J. H. Reed, and T. S. Rappaport, "Geometrical-based statistical macrocell channel model for mobile environments," *IEEE Trans. Commun.*, vol. 50, no. 3, pp. 495–502, Mar. 2002.
[16] L. Talbi and G. Y. Delisle, "Experimental characterization of EHF multipath indoor radio channels," *IEEE J. Sel. Areas Commun.*, vol. 14, no. 3, pp. 431–440, Apr. 1996.
[17] L. Talbi, "Spatial and temporal variations of the indoor wireless EHF channel," *Wireless Pers. Commun.*, vol. 23, no. 1, pp. 161–170, Oct. 2002.
[18] M. C. Greenberg, K. L. Virga, and C. L. Hammond, "Dual exponential tapered slot antenna (DETSA) characterstics," *IEEE Trans. Veh. Technol.*, vol. 52, pp. 305–312, Mar. 2003.
[19] T. M. Cover and J. A. Thomas, *Elements of Information Theory*. New York: Wiley, 1991.

Nathan A. Goodman (S'98–M'02) received the B.S., M.S., and Ph.D. degrees in electrical engineering from the University of Kansas, Lawrence, in 1995, 1997, and 2002, respectively.

He is currently an Assistant Professor in the Department of Electrical and Computer Engineering at the University of Arizona, Tuscon. Within the department, he directs the Laboratory for Sensor and Array Signal Processing. From 1996 to 1998, he was an RF Systems Engineer for Texas Instruments, Dallas, TX, and from 1998 to 2002, he was a Graduate Research Assistant in the Radar Systems and Remote Sensing Laboratory (RSL) at the University of Kansas. His research interests are in radar and array signal processing.

Dr. Goodman was awarded the Madison A. and Lila Self Graduate Fellowship from the University of Kansas in 1998. He was also awarded the IEEE 2001 International Geoscience and Remote Sensing Symposium Interactive Session Prize Paper Award.

Kathleen L. Melde (previously Kathleen L. Virga) (S'85–M'87–SM'97) received the B.S. degree from California State University, Long Beach, in 1985, the M.S. degree from California State University, Northridge, in 1987, and the Ph.D. degree from the University of California, Los Angeles, in 1996, all in electrical engineering. Her dissertation involved the modeling of broadband and integrated antennas for wireless communications.

From 1985 to 1996, she worked in the Radar Systems Group at Hughes Electronics in El Segundo, CA. Her work experience includes diverse projects in the Electromagnetic Systems Laboratory and Solid State Microwave Laboratories of the Radar and Communications Sector. She has made contributions to the design and development of phase shifters, RF feed networks, radiator elements and transmit/receive (T/R) modules for airborne phased and active array programs. She has extensive experience in modeling, fabrication and measurement of the performance of antennas, antenna arrays, high-density microwave circuits, and high-speed packaging interconnects. She was a task leader for several internal research and development projects. In 1996, she joined the electrical and computer engineering faculty at the University of Arizona, Tucson. Her current research interests involve applied electromagnetics, antenna theory and design, and microwave circuit design. Her current projects involve array antennas, antenna element design and characterization, wireless propagation, high speed electronic packaging, and the development of circuits for intelligent RF front ends. She has over 60 publications and 4 U.S. patents. She has been an expert witness and consultant in the area of RF circuits and antennas.

Dr. Melde is a member of the International Radio Science Union (URSI), Eta Kappa Nu, Tau Beta Pi, and Sigma Xi. She has received numerous awards such as the Hughes Aircraft Company Doctoral Fellowship, a UCLA Department of Electrical Engineering Graduate Woman of the Year award, and was a finalist for the URSI Student Competition. She has been an invited keynote speaker on several occasions such as the California State University Northridge, School of Engineering Commencement. She is a member of the Antennas and Propagation (AP-S) and Microwave Theory and Techniques (MTT) Societies. From 1999–2001 she served on the administrative committee (AdCom) for the IEEE AP-S Society. She is an Associate Editor for the IEEE TRANSACTIONS ON ANTENNAS AND PROPAGATION and a reviewer for several IEEE journals. She serves on the Technical Program Committee for the annual IEEE International Symposiums on Antennas and Propagation.